

# Can the charged Higgs boson be discovered in $e\gamma$ collisions using the channel $e^-\gamma \rightarrow \nu H^-$ ?

Shinya Kanemura

Physics and Astronomy Department, Michigan State University  
East Lansing, MI 48824-1116, USA

Kosuke Odagiri

Theory Group, KEK, 1-1 Oho, Tsukuba, Ibaraki 305-0801, Japan

## Abstract:

We consider the single production of charged Higgs bosons  $H^\pm$  of the two-Higgs-doublet model in  $e\gamma$  collisions through the production subprocess  $e^-\gamma \rightarrow \nu H^-$ . As the production rate is governed by the size of the loop-induced  $H^\pm W^\mp \gamma$  coupling, the cross section can only be substantial for smaller values of  $\tan\beta$ ,  $\tan\beta \lesssim 1$ , where the top-bottom loop contribution is enhanced. In this case, however, the natural width of the charged Higgs boson becomes large so that the Standard Model continuum background becomes important. We study the background subprocess  $e^-\gamma \rightarrow \nu \bar{t} b$  including the interference with the signal, and find that in the region of charged Higgs mass that can be interesting, the signal is difficult to detect.

Multi-doublet Higgs sectors arise naturally in several extensions of the Standard Model (SM) including the Minimal Supersymmetric Standard Model (MSSM), and these give rise to the charged Higgs boson  $H^\pm$ . Its discovery at present and future collider experiments has been the subject of much debate<sup>1</sup>, but it remains that the large mass region is elusive.

Here we study the single production channel,

$$e^-\gamma \rightarrow \nu H^-, \quad (1)$$

in the  $e\gamma$  option of future linear colliders. The process involves the  $H^\pm W^\mp \gamma$  vertex [2] which is forbidden at tree level because of gauge invariance, and is therefore loop-induced. The main motivation for considering this process is as a discovery mode. Although the physics potential of the  $e\gamma$  option is limited compared to the  $e^+e^-$  and  $\gamma\gamma$  options, it is possible that earlier experiments

---

<sup>1</sup>See ref. [1] and the references therein for a review of the current status.

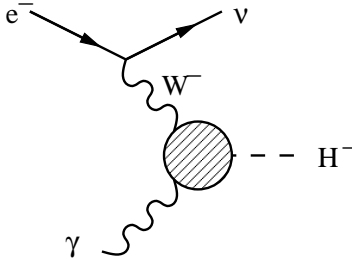


Figure 1: The Feynman graph for the signal process

find one or more of the neutral Higgs bosons and the measurements indicate the presence of a heavy charged Higgs boson in the parameter region that is accessible using the above channel. For this reason it is important to have a grasp of the accessibility of the  $e^- \gamma \rightarrow \nu H^-$  channel and the parameter regions in which it is applicable.

To be more specific, we want to find out whether a charged Higgs boson heavier than a half of the  $e^+e^-$  centre-of-mass energy can be produced in the  $e^- \gamma$  environment for values of  $\tan \beta$  and other parameters which are inaccessible through the  $e^+e^-$  single charged Higgs production modes studied in ref. [1].

For evaluating the signal cross section we utilised the form factors as given in ref. [3]. Out of the three form factors describing the  $H^\pm W_\mu^\mp \gamma_\nu$  vertex, only two are independent by gauge invariance such that the vertex is written as:

$$V^{\mu\nu} = G \frac{-p_\gamma \cdot p_W g^{\mu\nu} + p_\gamma^\mu p_W^\nu}{m_W^2} + iH \frac{p_\gamma^\rho p_W^\sigma \varepsilon^{\mu\nu\rho\sigma}}{m_W^2}. \quad (2)$$

Our convention is  $\varepsilon_{0123} = 1$ . Our spin averaged matrix element squared, corresponding to the Feynman diagram of figure 1, is given by:

$$|\overline{\mathcal{M}}|^2 = \left( \frac{e^2 \sqrt{-\hat{t}}}{4m_W \sin^2 \theta_W (\hat{t} - m_W^2)} \right)^2 [\hat{s}^2 |G - H|^2 + \hat{u}^2 |G + H|^2]. \quad (3)$$

where  $\hat{s}, \hat{t}$  and  $\hat{u}$  are the usual Mandelstam variables for the subprocess.

The form factors  $G$  and  $H$  were calculated in the two-Higgs-doublet model (2HDM) with softly broken discrete symmetry. For the Yukawa interaction of quarks, we have adopted the so-called Type II coupling [4]. For the fermionic loops, we only include the top-bottom contributions.

For the Standard Model parameters, we followed the values in ref. [1]. For the parameters of the 2HDM Higgs sector, we chose  $\alpha = \beta - \frac{\pi}{2}$ ,  $m_{h^0} = 120$  GeV,  $m_{H^0} = \sqrt{m_{H^\pm}^2 + m_W^2}$ ,  $m_{A^0} = \sqrt{m_{H^\pm}^2 - m_W^2}$ , and  $\mu = m_{A^0}$ .  $\alpha$  is the mixing angle between CP-even neutral Higgs bosons.  $m_{h^0}$ ,  $m_{H^0}$  and  $m_{A^0}$  are the masses of the lighter and heavier CP-even Higgs bosons  $h^0, H^0$  and the CP-odd Higgs boson  $A^0$ , respectively.  $\mu$  is the soft-breaking mass parameter for

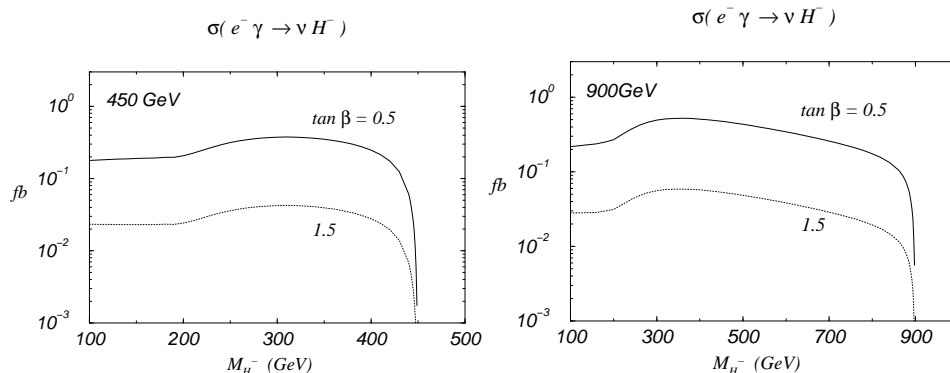


Figure 2: The signal cross section at  $\sqrt{\hat{s}} = 450$  GeV (left) and  $\sqrt{\hat{s}} = 900$  GeV (right).

the discrete symmetry. This parameter choice corresponds to the MSSM Higgs sector in the large  $m_{H^\pm}$  limit.

Figure 2 shows the total signal cross section at two values of subprocess centre-of-mass energy  $\sqrt{\hat{s}}$ , 450 GeV and 900 GeV. These roughly correspond to  $e\gamma$  collisions using Compton back-scattered photons from a  $e^+e^-$  collider at  $\sqrt{s} = 500$  GeV and 1 TeV. We have omitted the photon structure function for simplicity and in order that the physics of the process becomes more clear. The effect of this convolution with the photon structure function is that the large mass end of the distribution is suppressed, and the rise of the cross section in the medium mass range is counteracted, such that the distributions shown in figure 2 become more ‘flat’ as seen in figure 8 of ref. [5].

We show the rates for two values of  $\tan\beta$  at 0.5 and 1.5. As the dominant part of the cross section comes from the top-bottom loops, the  $\tan\beta$  dependence is mainly due to the Yukawa coupling and the chirality structure of the  $H^\pm W^\mp \gamma$  vertex. In the large and small  $\tan\beta$  regions, the  $\tan\beta$  dependence is approximately as follows:

$$\sim m_W^4 \cot^2 \beta \left( \tan \beta \ll \frac{m_t}{m_b} \right), \quad \text{and} \quad \sim m_W^4 \frac{m_b^4}{m_t^4} \tan^2 \beta \left( \tan \beta \gg \frac{m_t}{m_b} \right). \quad (4)$$

The enhancement of the cross section in the large  $\tan\beta$  region is negligible. The Higgs and gauge boson contributions are small when the cross section is substantial. We have explicitly confirmed that other combinations of Higgs parameters do not affect the rate significantly. This is a reflection of the fact that there are no  $\mathcal{O}(M^2/m_W^2)$  terms in the  $H^\pm W^\mp \gamma$  vertex due to gauge invariance, and only  $\mathcal{O}(\ln M^2)$  terms contribute for large  $M$ .  $M$  represents the characteristic mass of the particles in the loop.

From this  $\tan\beta$  dependence, it follows that if we adopt the MSSM parameters based on the LEP constraints [6] which give  $\tan\beta \gtrsim 3$ , the signal is too small to be observable. The  $e\gamma$  integrated luminosity is typically  $\sim 100 \text{ fb}^{-1}$  [7].

The cross section rises slowly with increasing  $\sqrt{\hat{s}}$  as  $\ln(\hat{s}/m_W^2)$ , as this is a  $t$ -channel process. Our results are substantially smaller than the case of neutral Higgs boson production considered in ref. [8]. The case of neutral Higgs boson production is dominated by the low  $p_T$  photon-fusion contributions, such that the cross section scales as  $\ln(\hat{s}/m_e^2)$ .

In the heavy  $H^\pm$  region which is the main interest of our study, the branching ratio for the mode  $H^- \rightarrow \bar{t}b$  is practically 100% especially at small  $\tan\beta$ . We do not consider other decay modes as they offer no advantage compared to this mode. For the production process (1) and the  $\bar{t}b$  decay mode, there is irreducible background coming from the Standard Model continuum production:

$$e^- \gamma \rightarrow \nu \bar{t} b. \quad (5)$$

We evaluated this background, as well as its interference with the signal which we discuss later on, using HELAS [9]. The Feynman diagrams for this process are shown in figure 3. The numerical integrations were carried out using a combination of Simpson's rule and naive Monte Carlo. We set all widths to

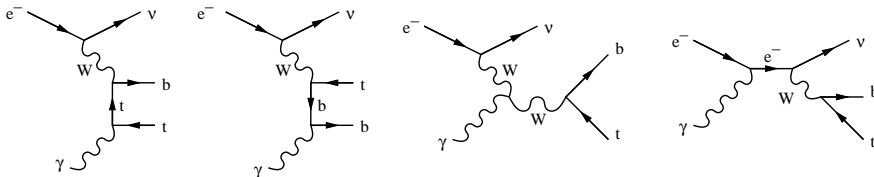


Figure 3: The Feynman graphs for the background process

zero, except for the natural width of the charged Higgs boson  $\Gamma_{H^\pm}$  which affects the calculation of the signal and the signal-background interference.

The total rate for the background at  $\sqrt{\hat{s}}$  of 450 GeV and 900 GeV are 28.4 fb and 69.2 fb, respectively. However, these numbers are not very meaningful as the dominant part of the background cross section comes from regions where the bottom quark is collinear with the initial photon direction. In order to have a more meaningful comparison with the signal cross section we introduced a cut on the bottom quark  $p_T$  at 50 GeV and 100 GeV respectively for the two collider energies. We have explicitly verified that our main conclusions are independent of the value of this cut-off. The background cross sections drop to 3.5 fb and 11.8 fb, respectively, and the resulting  $\bar{t}b$  invariant mass distributions are shown in figure 4. The binning width is 20 GeV.

20 GeV is a pessimistic estimate for the mass reconstruction resolution so that, had the widths been dominated by the detector resolution, it would be meaningful to compare the numbers from figure 2 directly with those on figure 4. One may thereupon conclude for instance that for  $\tan\beta = 0.5$ ,  $m_{H^\pm} = 700$  GeV and  $\sqrt{\hat{s}} = 900$  GeV, the signal and background rates are both about 0.3 fb so that for an integrated luminosity of  $100 \text{ fb}^{-1}$  and an optimistic value for the acceptance rate of about 25% let us say, there would be a nearly  $3 \sigma$  signal.

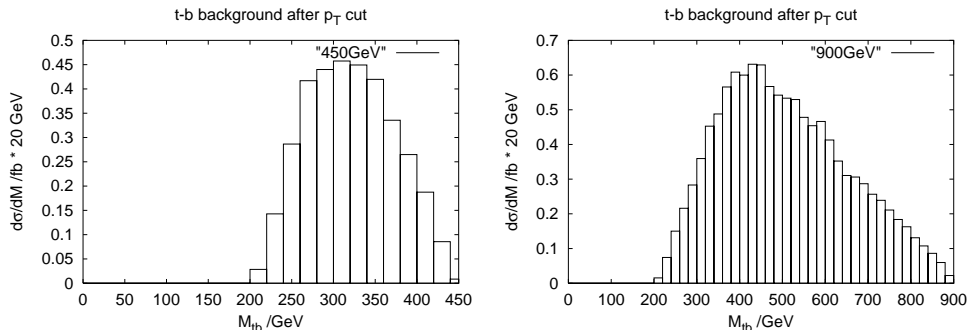


Figure 4: The background cross section at  $\sqrt{\hat{s}} = 450$  GeV (left) and  $\sqrt{\hat{s}} = 900$  GeV (right).

However, this is not the case as when  $\tan \beta$  is small and the signal is large, the natural width  $\Gamma_{H^\pm}$  also becomes large. For the case  $\tan \beta = 0.5$  and  $m_{H^\pm} = 700$  GeV, the width due to the  $\bar{t}b$  decay is about 150 GeV. What happens here is that the signal and the decay width both behave as  $\cot^2 \beta$  at low  $\tan \beta$  such that the signal distribution in  $M_{\bar{t}b}$  near  $m_{H^\pm}$  remains constant when  $\tan \beta$  is varied. Hence S/B, the signal over the continuum background integrated over the resonant region, remains constant as a function of  $\tan \beta$ . However, the total number of signal events does increase at low  $\tan \beta$  such that the signal significance, defined by  $S/\sqrt{B}$  over the resonant region, does improve at low  $\tan \beta$ .

Let us adopt the naive approach, which we nevertheless believe gives a good estimate of the full result, in which we define the cross section over the resonant region by:

$$\sigma_{\text{resonance}} = \left. \frac{d\sigma}{dM_{\bar{t}b}} \right|_{M_{\bar{t}b}=m_{H^\pm}} \times \Gamma_{H^\pm}. \quad (6)$$

We also include the effect of the interference between the signal and the background in order to have a consistent description of the production process. This definition circumvents the complications associated with the treatment of the signal when the charged Higgs boson is significantly off-shell. For a signal that has a pure Breit-Wigner distribution, (6) gives a rate that is too small by factor  $\pi/2$ . Our argument is that we are only interested in the resonant region whose width is given by  $\Gamma_{H^\pm}$ . We note that this approach gives a somewhat optimistic estimate, where it is assumed that both the signal and the background are nearly flat over the resonant region whereas the signal is peaked when  $H^\pm$  is on-shell. We also note that this naive approach becomes questionable when the width becomes comparable with the characteristic mass scale. However, our goal in this study is merely to establish whether, and in what region of the phase space, the signal process (1) can be seen.

S/B remains almost constant as a function of  $\tan \beta$  as mentioned before, so that we can do this calculation for any small  $\tan \beta$ . We adopt the value

$\tan\beta = 0.5$ , and in table 1 we show the total rate against the SM expectation over the resonant region as defined above. This value of  $\tan\beta$  is near the lowest bound acceptable from the criterion of the validity of perturbation theory [10].

$M_{H^\pm}$ /GeV	$\Gamma_{H^\pm}$ /GeV	total /fb	background /fb
250	15.7	0.36	0.23
300	31.6	0.94	0.75
350	47.6	1.13	0.97
400	63.2	0.78	0.70

$$\sqrt{\hat{s}} = 450 \text{ GeV}$$

$M_{H^\pm}$ /GeV	$\Gamma_{H^\pm}$ /GeV	total /fb	background /fb
300	31.6	0.66	0.51
400	63.2	2.17	2.05
500	93.0	2.90	2.87
600	121.	2.45	2.52
700	149.	2.07	2.14
800	175.	1.19	1.25

$$\sqrt{\hat{s}} = 900 \text{ GeV}$$

Table 1: Total rate versus the expected background rate over the resonant region, as defined in the text, at two centre-of-mass energies, after the  $p_T$  cut. The numbers shown are for  $\tan\beta = 0.5$ .

From the numbers shown in table 1, we point out the following. First, let us consider the  $e\gamma$  integrated luminosity of  $100 \text{ fb}^{-1}$  per year and an acceptance rate of few times 10%. For concreteness let us adopt 25% for example as an optimistic estimate. We see that the signal significance, defined as  $S/\sqrt{B}$  with  $S$  being defined here as the total rate minus the background rate, is at most about  $1.25\sigma$  at  $\sqrt{\hat{s}} = 450 \text{ GeV}$  and  $1\sigma$  at  $\sqrt{\hat{s}} = 900 \text{ GeV}$ . Even with increased acceptance rate and increased luminosity, the channel is not useful for discovery in this model or generally in the 2HDM.

Second, the interference between the signal and the background is negative and sometimes large. In fact, there are regions where the total rate is smaller than the expected background. This is explained as follows. According to the definition of equation (6), it is easy to see that the interference between the signal and the background is due to the imaginary part of the form factors  $G$  and  $H$  given in equation (2). The imaginary parts of the top-bottom loop contributions in these form factors have exactly the form that comes from the interference between the continuum background and the decay  $H^- \rightarrow \bar{t}b$ . Thus it is possible to relate the magnitude of the interference term to the signal, and it turns out that the contribution of the interference term is of the same order and has the sign that is opposite to the signal.

Lastly, we note that in this model the channel seems to offer no advantage

compared to  $W^\pm H^\mp$  associated production in the  $e^+e^-$  mode [1, 3, 11].

The extension of our calculation by the inclusion of other light fermions into the loop can not improve the situation as whatever increases the signal rate also increases the charged Higgs boson width while the branching ratio into  $t\bar{b}$  in general falls. On the other hand, by the inclusion of new heavy virtual particles in the  $H^\pm W^\mp \gamma$  vertex that have large non-decoupling contributions, it is possible that the signal cross section is enhanced significantly without enhancing the width. This may be possible if we consider non-decoupling contributions from heavy squarks with large left–right mixings in the stop sector, and in this case, there is some discovery potential for this mode.

In this paper we did not discuss the decay of the top quark. The polarisation of the top quark is opposite between the signal and the background in the limit  $M_{H^\pm} \gg m_t$ , but the statistics is presumably too low to utilise polarisation analysis as described in ref. [12]. We should also mention that in our study we have neglected the reducible background from the top pair production subprocess  $e^- \gamma \rightarrow e^- t\bar{t}$ . This could very well be important. The consideration of these more detailed points is expected to make signal detection even more difficult.

To conclude, we have considered the process  $e^- \gamma \rightarrow \nu H^-$  as a discovery mode for the charged Higgs boson at the  $e\gamma$  option of future linear colliders. Although the signal evaluated in the 2HDM can reach reasonable rates for  $\tan \beta \lesssim 1$ , the background is large and it is difficult to see the charged Higgs boson through this channel.

Finally, we acknowledge advice and technical help from Stefano Moretti. We also thank Yasuhiro Okada, Wayne Repko and C.-P. Yuan for enjoyable discussions. We are grateful for the financial support from KEK which made this collaboration possible.

## References

- [1] S. Kanemura, S. Moretti and K. Odagiri, *J. High Energy Phys.* **02** (2001) 011.
- [2] M. Capdequi Peyranère, H.E. Haber, P. Irulegui, *Phys. Rev.* **D 44** (1991) 191.
- [3] S. Kanemura, *Eur. Phys. J.* **C 17** (2000) 473.
- [4] J.F. Gunion, H.E. Haber, G.L. Kane and S. Dawson, ‘The Higgs Hunters Guide’, Addison Wesley Publishing Co. (1990).
- [5] S. Kanemura, S. Moretti and K. Odagiri, preprint CERN–TH/2001–064, KEK–TH–757, MSUHEP–01042, hep-ph/0004180.
- [6] ALEPH Collaboration, *Phys. Lett.* **B 495** (2000) 1; L3 Collaboration, *Phys. Lett.* **B 495** (2000) 18.
- [7] For the TESLA design, see, e.g.: [http://www.desy.de/~njwalker/ecfa-desy-wg4/parameter\\_list.html](http://www.desy.de/~njwalker/ecfa-desy-wg4/parameter_list.html).

- [8] D.A. Dicus and W.W. Repko, *Phys. Rev. D* **53** (1996) 3616;  
Y. Liao and W.W. Repko, *Phys. Rev. D* **57** (1998) 1.
- [9] H. Murayama, I. Watanabe and K. Hagiwara, KEK Report 91-11, January 1992.
- [10] S. Kanemura, T. Kasai and Y. Okada, *Phys. Lett. B* **471** (1999) 182.
- [11] S.H. Zhu, preprint January 1999, hep-ph/9901221;  
A. Arhrib, M. Capdequi Peyranère, W. Hollik, G. Moulhaka, *Nuc. Phys. B* **581** (2000) 34.
- [12] K. Odagiri, *Phys. Lett. B* **452** (1999) 327.